

# The color signature of the transit of HD 209458: discrepancies between stellar atmospheric models and observations

B. Tingley<sup>1,2</sup>, C. Thurl<sup>1,2</sup>, and P. Sackett<sup>1,2</sup>

<sup>1</sup> Research School of Astronomy and Astrophysics, ANU Cotter Road, Weston, Canberra ACT 2611, Australia

<sup>2</sup> ANU Planetary Science Institute c/o Mount Stromlo Observatory, Cotter Road, Weston ACT 2611, Australia  
e-mail: [tingley;cthurl]@mso.anu.edu.au; Penny.Sackett@anu.edu.au

Received 29 August 2005 / Accepted 22 October 2005

## ABSTRACT

Exoplanetary transits produce a double-horned color signature that is distinct from both binaries and blends and can thus be used to separate exoplanets from false positives in transit searches. Color photometry with precision sufficient to detect this signal in transits of HD 209458 is available in the literature. Analysis of these observations reveals that, while the signature does exhibit the expected shape, it is significantly stronger than PHOENIX atmospheric models predict.

**Key words.** stars: planetary systems – occultations, stars: atmospheres

## 1. Introduction

The radial velocity technique is most commonly used technique for the classification of transiting exoplanet candidates. It measures the velocity shift of the parent star, which allows estimates the mass of the transiting companion via observations of a radial velocity shift in the lines of the host star. However, this technique is not ideal. Not only is it time- and resource-consuming, but it fails to classify some candidates. These unclassifiable candidates can be either too faint to be observed with the precision necessary to identify the signal, too active to allow the signal to be identified over the stellar noise, or are actually blends. In many cases, blends leave no spectral fingerprint and thus cannot be discerned from the other phenomena and represent the greatest obstacle to transit surveys with the potential to discover terrestrial planets.

Other techniques exist to make this classification. The Rossiter-McLaughlin effect manifests itself as a perturbation of the radial velocity of the parent star during a transit, allowing the transiting body to be classified (Worek 2000). However, it does suffer from most of the same problems as the radial velocity technique. Seager & Mallén-Ornelas (2003) describe a technique that analyzes the shape of the transit to determine the mass of the transiting body, for which blends produce anomalous results. This technique requires high-precision photometry and utilizes assumptions about the mass-radius relationship for the lower main sequence, which do not necessarily hold in all cases. Torres et al. (2004) propose a technique involving detailed modelling of the full light curve to

test blend scenarios, which helped in identifying OGLE-TR-33 as a blend.

The color change exhibited by the central star during transit can also be used to make this classification, as exoplanets, grazing binaries and blends all have own, distinct color signature. First realized by Rosenblatt (1971) and further developed by Borucki & Summers (1984) and discussed in connection with hot Jupiters by Sackett (1999), a non-grazing exoplanetary transit will exhibit a sharply peaked double-horned color profile, which models predict will have an amplitude on the order of 10% of the transit depth. This is markedly different from the broad, single-peaked profiles of binary stars and blends (Tingley 2004). The strengths and shapes of these signatures are highly dependent on various factors: the differential limb darkening between wavebands, orbital characteristics, the relative sizes of the transiting objects and the color differences between the eclipsing (normally a background eclipsing binary star) and constant (non-eclipsing) components.

Given that typical giant exoplanet transits have a depth of 1–2% percent, exoplanetary color signatures should be on the order of a few millimag. At present, good ground-based photometry can have a precision better than 1 millimag per observation (see, for example, Jha et al. 2001). This means that these signatures should be observable from the ground and should therefore be present in high precision multi-color observations of the transit of HD 209458 already available in the literature. The photometric possibilities from space are even more promising. Precisions approaching 0.1 mmag are possible (Brown et al. 2001) with existing instruments, which can help to verify the strength of the signature. In the absence of

suitable ground-based data, this can be used to establish if the signature is detectable with ground-based photometry.

## 2. Photometry of the transit of HD 209458

Three different sets of observations of HD 209458 are available in the literature that have sufficient precision to be useful for this study: the HST observations of Brown et al. (2001), the simultaneous Stromgren photometry of Deeg et al. (2001), and the *BVIRZ* observations of Jha et al. (2001).

### 2.1. HST observations

In 2000, the HST was utilized in an unprecedented fashion in order to obtain extremely high precision photometry of the HD 209458 transit. By using the Space Telescope Imaging Spectrograph (STIS) on a small, relatively featureless portion of the spectrum (from 5813 to 6382 Angstroms), Brown et al. (2001) were able to obtain a photometric precision of  $1.1 \times 10^{-4}$  per sample, with one sample every 80s, for the transit of HD 209458. This surpasses the capabilities of any ground-based instrument by a factor of approximately ten. However, the observations were taken only in this single passband, and so alone cannot be used to identify a color change during the transit. The authors did split their spectrum into “red” (the reddest 300 Angstroms) and “blue” (the bluest 300 Angstroms) and noted that a feature was present in the “red”–“blue” color. The weakness of the signature is directly attributable to the fact that there is little wavelength separation in this “color”. However, when combined with ground-based data, the extremely high precision and temporal coverage of the HST data allows the color signatures to be assessed and analyzed.

### 2.2. Observatorio Sierra Nevada observations

Another useful data set was created by Deeg et al. (2001), which contains simultaneous Stromgren  $u$ ,  $v$ ,  $b$  and  $y$  photometry using the 0.9 m telescope at the Observatorio Sierra Nevada in Spain. After sigma-clipping, this data set includes 129 in-transit plus 29 out-of-transit observations in all bands. The precision of these data was about 4 mmag in  $u$  and  $y$  and 2 mmag in  $v$  and  $b$ , as measured from the out-of-transit scatter. While the data are of excellent quality, the two filters with the highest precision do not have a large separation in wavelength, with only 600 Angstroms between  $v$  and  $b$ . Moreover, there appears to be some systematic noise present, which is most prominent in  $u$  and  $y$ , less so in  $b$  and almost non-existent in  $v$ . Readily visible in Fig. 1 of Deeg et al. (2001), these variations are sufficiently strong to obscure the expected exoplanetary signature in all but  $v$ .

### 2.3. Hawai'i 2.2 m and Hawaii 0.6 m observations

Useful observations from the University of Hawai'i 2.2 m and 0.6 m were published by Jha et al. (2001). They include  $B$ ,  $V$ ,  $I$ ,  $R$  and  $Z$  photometry of a transit of HD 209408 in 1999, with precisions of 0.8 mmag, 1.6 mmag, 1.2 mmag and 0.8 mmag respectively. The event was observed 43 times in  $B$  from the

Hawaii 0.6 m and 17 times in each of the other filters from the Hawaii 2.2 m. This data set had the potential to be the most useful, as it is comprised of simultaneous, high-precision photometry through multiple filters with broad separation in wavelength. The purpose of the Jha et al. project, however, was to observe slight differences in transit depth in different bands, in order to get a better estimate of the radius of HD 209458b. As such, the data do not capture the ingress of the transit and additionally have poor time resolution. These factors mean that these data are unsuitable for the identification of a color signature that occurs over relatively short time scales, especially considering that the observations alternated filters and switched to comparison stars. The lack of an ingress makes it hard to compare these data with other data sets, as systematic errors can easily produce a single horn in color typical of those caused by an exoplanet during ingress/egress. The presence of a second horn at the proper time is a necessary verification.

## 3. Modeling

The atmosphere of HD 209458 was modeled using state-of-the-art PHOENIX grid models (v. 2.6) (Hauschildt et al. 1999, Hauschildt, Allard & Baron, 1999, Hauschildt & Baron 1999) obtained through an ongoing collaboration with Peter H. Hauschildt. PHOENIX models show significantly different limb darkening behavior than that described by analytic limb darkening laws (Bryce et al. 2002; Claret 2003). The models used to fit the transit are one-dimensional, assume Local Thermodynamic Equilibrium (LTE) and use spherically-symmetric radiative transfer and dynamic opacity sampling. The intensity profile is calculated with a wavelength resolution of  $\leq 1 \text{ \AA}$  at 99 angular points. These points are distributed evenly in  $\cos \theta$  for most of the inner parts of the stellar disk, where  $\theta$  is the emergent angle. However, angular sampling increases toward the limb, where greater changes in the intensity profile occur.

The model atmospheres were generated for several different effective temperatures (5900 K, 6000 K, 6100 K), surface gravities ( $\log g = 4.0, 4.5$ ) and metallicities ( $-0.5, 0.0, +0.5$ ). The model atmospheres were converted to limb darkening profiles by convolving the stellar intensity profiles with the appropriate filter passbands. The limb-darkening profiles were then used to create modeled transit shapes, leaving the exoplanet-star radius ratio ( $\frac{R_p}{R_*}$ ), the impact parameter ( $i_p$ ) (the distance from center of the star to the point of nearest approach of the exoplanet's projected path across the disk of the star, in units of stellar radii) and the duration of the transit as free parameters. The code that modeled the transits was designed to include sub-pixels to minimize the effects of pixellation on the limbs of the exoplanet and star. This may otherwise cause small but noticeable errors. A simple  $\chi^2$  minimalization was used to find the best-fit model to the HST data. The observed properties of HD 209458 are uncertain:  $([\text{Fe}/\text{H}] = 0.00 \pm 0.02, M_* = 1.1 \pm 0.1 M_\odot$  and  $R_* = 1.2 \pm 0.1 R_\odot$ , which yield  $\log g = 4.36 \pm 0.05$ ,  $T_{\text{eff}} = 6000 \text{ K} \pm 50 \text{ K}$  (Mazeh et al. 2000). Other groups have found slightly different values: Cody & Sasselov (2002) reported  $M_* = 1.06 \pm 0.11 M_\odot$  and  $R_* = 1.18 \pm 0.12 R_\odot$ , which yield  $\log g = 4.32 \pm 0.09$ ), Fischer & Valenti (2005)

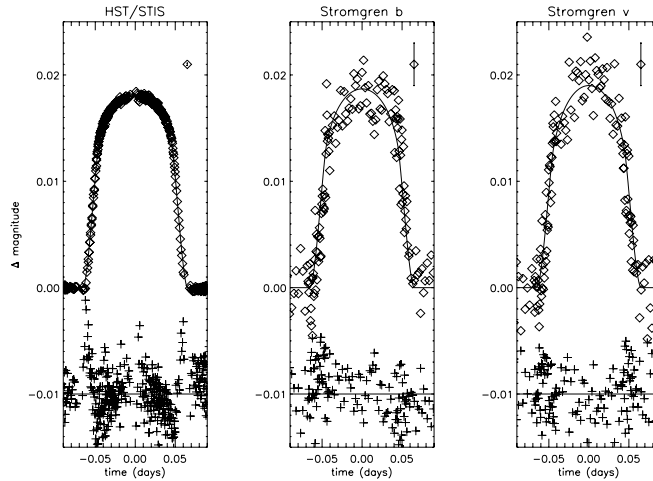


**Fig. 1.** Data (diamonds), the modeled fits (solid lines), residuals (crosses) are shown for the transit of HD 209458. Typical error bars are shown in the upper right hand corner of each plot. The model transits were determined by using the best fit of 362 models to the HST data. Note that there is still a small amount of symmetric residual in the HST fit, which has been increased by a factor of 10 for clarity. Note also the strongly asymmetric residual in the  $b$  passband, the cause of which is unknown.

reported  $M_* = 1.14 M_\odot$  and  $R_* = 1.12 R_\odot$  with an error in  $\log g$  of 0.06 dex, which yield  $\log g = 4.40 \pm 0.06$  and Valenti & Fischer (2005) reported  $[\text{Fe}/\text{H}] = +0.02 \pm 0.03$ . These values for  $\log g$  and  $[\text{Fe}/\text{H}]$  are all within nearly one sigma of one another and furthermore differences in these parameters at this level have a very small effect on transit shape – changing metallicity or temperature by 0.5 dex results in a change in a transit shape of less than 1% of the transit depth, while a similar change in surface gravity changes the shape by less than 0.1%. Therefore, it is reasonable to use intermediate values of temperature (5950 K, 6000 K, 6050 K) and surface gravity ( $\log g = 4.30, 4.36, 4.42$ ) to reflect these measurements and their uncertainties. These were then interpolated from the original models. The best-fit system parameters, using only the HST data as they are far more stable and precise than the Deeg data, were ( $T_{\text{eff}} = 6050$  K,  $[\text{M}/\text{H}] = -0.5$ ,  $\log g = 4.42$ ,  $R_p = 0.122 R_*$ ,  $i = 86.1^\circ$ ). The result of this analysis can be seen in Fig. 1 (fits to transit shape) and 2 (resulting modeled color change).

Since the LTE PHOENIX models produced a color signature that accurately described the shape but not the amplitude of the observed signature, we implemented a fully non-LTE PHOENIX model in order to study if this could explain the observed discrepancies. As the non-LTE models have an immense computational load, only one was created and compared to the LTE model with the same parameters. As can be seen in Fig. 3, a fully non-LTE model does exhibit a stronger color signature than an LTE model (solar metallicity,  $T_{\text{eff}} = 6000$  K, and  $\log g = 4.50$ , with planetary parameters  $R_p = 0.122 R_*$ ,  $i = 86.1^\circ$ ), but the difference is marginal compared to the differences between model and observations.

#### 4. Results

The data from Deeg et al. (2001) alone do not reveal the exoplanetary color signature. The  $u$  and  $y$  observations are too noisy, especially at the ingress and egress of the transit, which

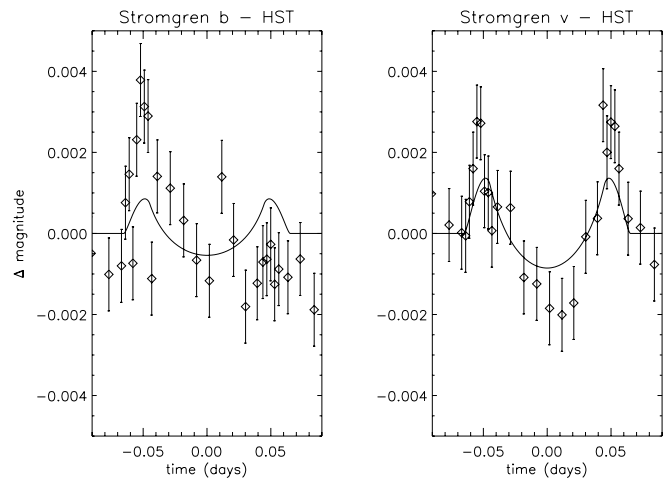


**Fig. 2.** This figure shows the  $b - HST$  and  $v - HST$  color change during the transit, along with the signatures from LTE PHOENIX models. Note that the systematic noise evident in  $b$  is also evident in the  $b - HST$  color change. The observed  $v - HST$  color change is very consistent in shape, if not in amplitude, to the model.

are most critical for this analysis. The  $b$  observations contain an asymmetric variation that is likely due to undetermined systematic effects. Only the  $v$  is sufficiently precise and stable. Moreover, even without the systematics in  $b$ , the  $b$  and  $v$  passbands (centered at  $4100 \text{ \AA}$  and  $4700 \text{ \AA}$  respectively) do not have enough chromatic separation to produce a strong signature. The expected signal in  $b - v$  from the models is less than 1 mmag from peak to trough. In principle, this is detectable with these data, given 145 observations with a precision in this color of approximately 3 mmag. However, the systematic noise obscures the faint expected signature.

The HST data must be combined with the Deeg data, therefore, to reveal the exoplanetary color signature. Figure 2 shows modeled and observed  $b - HST$  and  $v - HST$ . The  $b - HST$  shows a similar trend as observed in the residual for  $b$  in Fig. 1.

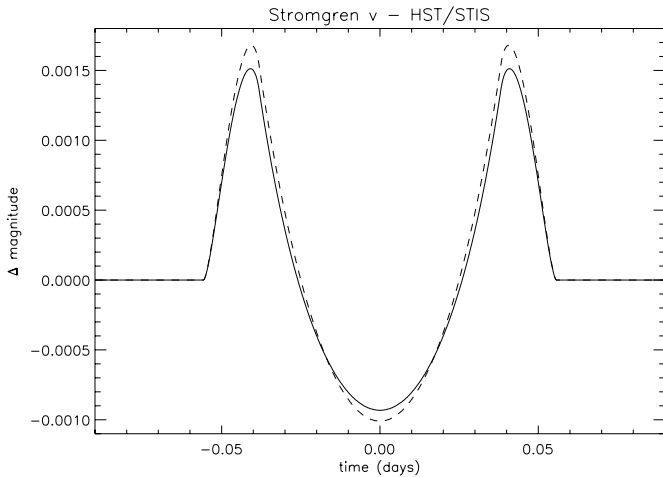


**Fig. 3.** This figure shows the  $v$ - $HST$  color change for a star with solar metallicity,  $T_{\text{eff}} = 6000$  K, and  $\log g = 4.50$ , with planetary parameters  $R_p = 0.122 R_*$ ,  $R_* = 1.36 R_J$  and  $i = 86.1^\circ$ . The solid line shows a model assuming LTE while the dashed line is a fully non-LTE model. Note that the latter demonstrates a stronger signature, yet still predicts a significantly weaker signature than the one observed.

The  $v$ - $HST$  plot clearly shows a color change that has a shape consistent with that predicted by the atmospheric models, but with a stronger amplitude. There was also some small amount of residual between the HST data and the model, visible in Fig. 1.

## 5. Conclusion

An exoplanetary color signature is clearly visible in the transit of HD 209458 in  $v - HST$ . Unfortunately, the data from Deeg et al. (2001) alone did not exhibit an exoplanetary signature, as the data were either too noisy or not separated enough in wavelength from the other passband. Even so, the signature that was detected using the HST data and the best of the ground-based data is strong enough that it could be observed from ground, in the absence of these systematics and in more widely separated passbands.

The color signature detected in the transit data of HD 209458 in our analysis was consistent in shape, but larger in amplitude than that expected using either LTE or fully non-LTE PHOENIX models, though the non-LTE models were superior. The detected signature was considerably stronger in  $v - HST/STIS$ , with an amplitude of approximately 5 mmag observed against 2.4 mmag predicted by the LTE model and

2.7 mmag predicted by the non-LTE model. This increases the viability of the color signature as a technique for classifying transit candidates, as the observed signature exceeds any prediction, being closer to 30% of the transit depth than 10%, the generally quoted valued.

The system parameters we derived are essentially identical to those found by Brown et al. (2001), despite the fact that they used a standard stellar limb darkening law, fitting its coefficients as free parameters. Thus the use of PHOENIX models does not adversely affect the estimation of transit parameters. The discrepancy in the amplitude of the color signature between the HD 209458 and PHOENIX models, suggests, if confirmed in other systems, that an important component to the factors that influence color near the stellar limb may still be absent in these models.

*Acknowledgements.* The authors would like to thank Peter Hauschildt, who provided his assistance and considerable expertise in the setting up of the PHOENIX models.

## References

- Borucki, W., & Summers, A. 1984, *Icarus*, 58, 121
- Brown, T. M., Charbonneau, D., Gilliland, R. L., Noyes, R. W., & Burrows, A. 2001, *ApJ*, 552, 699
- Bryce, H. M., Hendry, M. A., & Valls-Gabaud, D. 2002, *A&A*, 388, L1
- Claret, A. 2003, *A&A*, 401, 657
- Cody, A. M., & Sasselov, D. D. 2002, *ApJ*, 569, 451
- Deeg, H. J., Garrido, R., & Claret, A. 2001, *NewA*, 6, 51
- Fischer, D. A., & Valenti, J. A. 2005, *ApJ*, 622, 1102
- Hauschildt, P. H., Baron, E., 1999, *J. Computational Appl. Math.*, 102, 41
- Hauschildt, P. H., Allard, F., Ferguson, J., Baron, E., & Alexander, D. R. 1999, *ApJ*, 525, 871
- Hauschildt, P. H., Allard, F., & Baron, E. 1999, *ApJ*, 512, 377
- Jha, S., Charbonneau, D., Garnavich, P. M., et al. 2000, *ApJ*, 540, L45
- Mazeh, T., Naef, D., Torres, G., et al. 2000, *ApJ*, 532, L55
- Rosenblatt, F. 1971, *Icarus*, 14, 71
- Sackett, P. D. 1999, in *Planets Outside the Solar System: Theory and Observations* (NATO-ASI), ed. J. M. Mariotti & D. Alloin (Dordrecht: Kluwer), 189
- Seager, S., & Mallén-Ornelas, G. 2003, *ApJ*, 585, 1038
- Tingley, B. 2004, *A&A*, 425, 1125
- Torres, G., Konacki, M., Sasselov, D. D., & Jha, S. 2004, *ApJ*, 614, 979
- Valenti, J. A., & Fischer, D. A. 2005, *ApJS*, 159, 141
- Worek, T. F. 2000, *IBVS*, 4838, 1